

The band structure of chemically ordered Co_3Pt

This article has been downloaded from IOPscience. Please scroll down to see the full text article.

1996 J. Phys.: Condens. Matter 8 1151

(<http://iopscience.iop.org/0953-8984/8/9/007>)

View [the table of contents for this issue](#), or go to the [journal homepage](#) for more

Download details:

IP Address: 171.66.16.208

The article was downloaded on 13/05/2010 at 16:19

Please note that [terms and conditions apply](#).

The band structure of chemically ordered Co₃Pt

G Morañtis, J C Parlebas and M A Khan

IPCMS (UMR 46 CNRS), GEMME, 23, rue du Loess, 67037 Strasbourg Cédex, France

Received 21 August 1995, in final form 29 November 1995

Abstract. Owing to surface diffusion, the molecular beam epitaxy (MBE) technique has made it possible to produce new binary alloy films by coevaporation on a single-crystal substrate in an ultrahigh vacuum. In this fashion, a hexagonal close-packed (hcp) structure of the Co₃Pt compound with ferromagnetic and chemical order has been discovered recently which was not previously known in the bulk alloy equilibrium phase diagram. Using a tight-binding linear muffin-tin orbital (TB-LMTO) method for the electronic structure of Co₃Pt, we treat first the reference case of the fcc L1₂ phase and then the hcp phase. In this last phase we consider both the standard DO₁₉ structure and a modified version of it. We perform the band-structure calculation in both the paramagnetic and ferromagnetic cases, and on the basis of a total energy calculation we arrive at the conclusion that the ferromagnetic phase of the DO₁₉ structure is the most stable.

1. Introduction

Nowadays the molecular beam epitaxy (MBE) technique of preparation has opened up an exciting way of exploring a new class of chemically ordered alloys. For example, during the elaboration of thin layers of binary alloys through an ultrahigh-vacuum (UHV) coevaporation on a single-crystal substrate, a suitable choice of the different growth parameters allows one to obtain low-temperature phases that cannot be observed in usual bulk materials due to a lack of diffusion in the bulk. This is true in particular for the Co–Pt system, and the existing bulk phase diagrams [1] can then be completed towards the low temperatures. Let us first recall that the Co–Pt bulk phase diagram presents a continuous series of solid solutions with ferromagnetic order up to 90 at.% Pt at room temperature [1, 2]. Also the existence of chemically ordered Co₃Pt, CoPt and CoPt₃ phases is already well known, respectively corresponding to L1₂, L1₀ and L1₂ phases, as in the prototype Cu–Au phase diagram. Moreover the Co–Pt chemical and magnetic phase diagram has been theoretically calculated by Sanchez *et al* [3]. However, only recently, a new hexagonal close-packed (hcp) structure has been synthesized in (relatively) thin-film form by Harp *et al* [4] and Maret *et al* [5], through the use of MBE, i.e. simultaneous molecular beam epitaxial deposition of both Co and Pt on a crystalline substrate; Maret *et al* used a Ru(001) buffer.

Measuring a series of photon-energy-dependent magneto-optical Kerr-effect (MOKE) spectra of various Co₃Pt films, grown at temperatures varying from 950 to 350 K, Harp *et al* [4] discovered that a hcp structure was the preferred state for low-temperature arrangement, typically below 750 K. In this case, a strong new MOKE feature of about 2 eV width and corresponding to a photon energy of about 3.2 eV was attributed to the presence of this new Co₃Pt phase and tentatively explained by interband optical transitions of about the same energy (i.e. 3.2 eV) around the Fermi level. Maret *et al* [5] also point out a

new hcp Co_3Pt phase with long-range chemical ordering along the [001] growth direction as well as a strong perpendicular magnetic anisotropy along the same ('*c*') axis. However, the detailed crystallographic structure of the hcp phase considered is not yet fully determined: it contains alternating planes A and B such that the percentage of Pt in those planes varies as a function of the growth temperature. Two extreme possibilities are that in one case both planes A and B have equal amounts of Pt and are called mixed planes (this Ni_3Sn -type structure is labelled DO_{19} [6, 7]), and in the other case all the Pt atoms appear in A planes whereas the B planes contain only Co atoms (this structure will be called 'modified DO_{19} ' or DO'_{19}).

In the present work we use a scalar-relativistic version of the tight-binding linear muffin-tin orbital (TB-LMTO) method [8, 9] to explore the electronic structure and the corresponding total energies of various Co_3Pt phases in order to shed some light onto the experimental situation. From the point of view of band-structure calculation there have been several results concerning ordered binary Co–Pt compounds [10–12]. However, mostly CoPt_3 has been studied [11, 12] and Co_3Pt has been treated only in its cubic symmetry form of L1_2 type [10]. Also it should be noted that the spin–orbit coupling acts more effectively in the 5d state of Pt atoms than in the 3d state of Co atoms. Hence we can expect a much more significant spin–orbit contribution from Pt in the case of Pt overlayers upon noble metals for instance [13], or even in the case of CoPt_3 [11] as compared to Co_3Pt compounds, which we are dealing with in the present paper. For Co_3Pt a fully relativistic calculation is certainly not as important as in the previously considered cases.

The paper is organized as follows. In section 2, we briefly recall some general remarks on our electronic structure calculations. Next, in order to obtain a basis for further comparison, we report (section 3) our band-structure result for the well known L1_2 phase of face-centred cubic (fcc) Co_3Pt which is stable at high temperature ($T > 800$ K). Then, in section 4, we present our calculation for the corresponding DO_{19} structure, whereas section 5 is devoted to its modified form DO'_{19} as we explained above. In section 6 we discuss our numerical results and compare them with a few available experimental data as well as theoretical studies. Unfortunately, as already mentioned, it is only for the L1_2 phase of Co_3Pt that calculations are available. Section 7 gives a few concluding remarks.

2. The method for the electronic structure calculation

For the electronic structure calculation, throughout the present paper we have used the TB-LMTO method [8, 9]. Also the exchange correlation effect is included in the computation through the local density approximation (LDA) [14]. For Co we consider only s, p and d orbitals for the corresponding nine valence electrons ($3d^7 4s^2 4p^0$), whereas for Pt the f orbitals are also included ($5d^9 6s^1 6p^0 5f^0$). This is true for all of the Co_3Pt structures considered.

In the atomic-sphere approximation (ASA) that we use in the present paper, the crystal is subdivided into overlapping Wigner–Seitz (WS) spheres, centred around each atomic position in the unit cell and with a total volume which equals the volume of the unit cell. All of the various crystallographic structures of Co_3Pt that we consider are sufficiently close packed for the ASA to be a good approximation. However, we should recall that some band-structure calculated results are dependent upon the choice of the Wigner–Seitz radius R_{WS} —for example, the magnitudes of the magnetic moments and charge transfer. Here, the R_{WS} are adjusted so as to minimize the overlapping between WS spheres (<15%). For the *k*-space integration by the tetrahedron method [15, 16], *N* *k*-points are used in the irreducible Brillouin zones corresponding to various structures ($N = 220, 192$ and 200 for

respectively $L1_2$, DO_{19} and DO'_{19} structures of Co_3Pt). This number of k -points is found to be sufficient for obtaining a completely converged result. Also, in the present paper all of the electronic energies are traced with reference to the Fermi energy E_F .

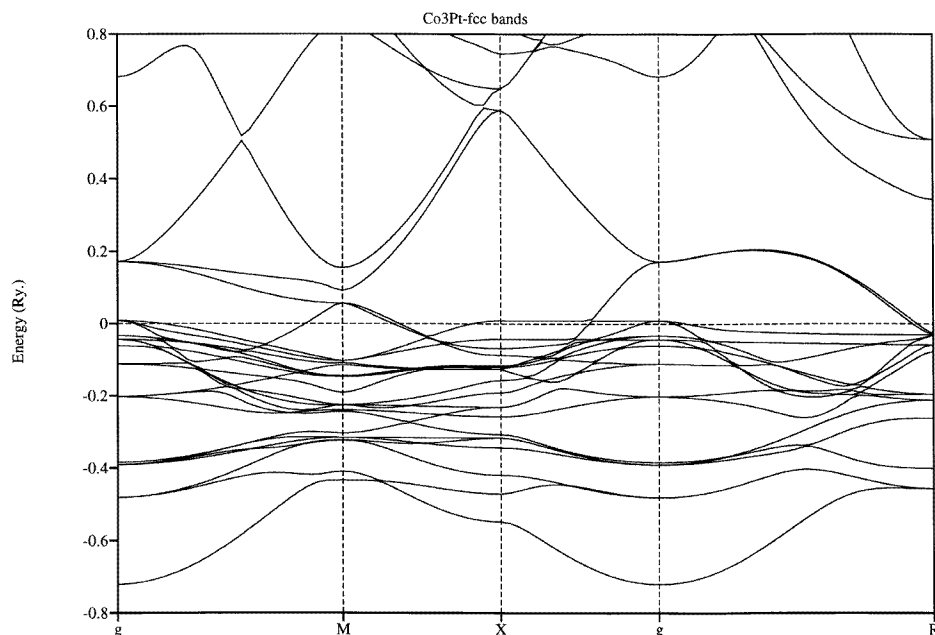


Figure 1. $L1_2$ Co_3Pt : energy bands along fcc high-symmetry directions in the paramagnetic phase.

3. The $L1_2$ structure of Co_3Pt

As for the $L1_2$ ordered structure of Co_3Pt (Cu_3Au -type), which is actually composed of four simple cubic sublattices, all of the (111) planes exhibit the same Co_3Pt composition. For this structure, the energy bands are given along characteristic high-symmetry directions in the paramagnetic phase (P)—see figure 1. For the ferromagnetic phase (F), the bands are about the same except that there is a downward and upward movement of majority and minority bands respectively. This movement is particularly pronounced for the bands lying near the Fermi level. This fact is revealed in the density of states (DOS) for the F phase in figure 2. Also, some physical quantities are presented in table 1, such as the DOS at the Fermi level, the number of states for each orbital of α origin ($\alpha = \text{Co}, \text{Pt}$), the charge variation ΔQ_α of a given α atom and the magnetic moment μ_α . Actually table 1 also contains similar results for the other structures of Co_3Pt , i.e. DO_{19} and DO'_{19} , which will be further presented in sections 4 and 5.

4. The DO_{19} structure of Co_3Pt

This structure is the tabulated Ni_3Sn hcp structure and the atomic positions are described in table 2 [6, 17, 18] with the following lattice parameters: $a = b = 5.189 \text{ \AA}$ and

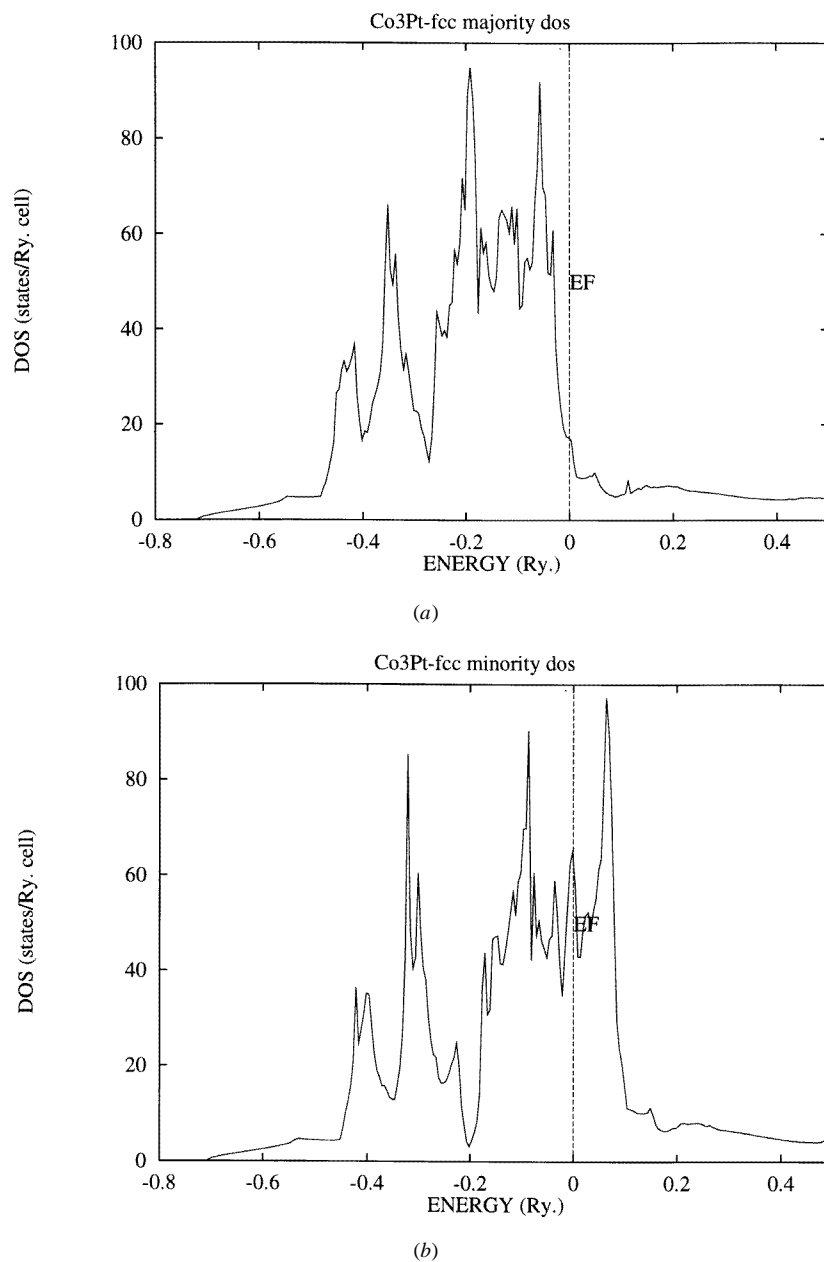


Figure 2. L₁₂ Co₃Pt: the total ferromagnetic DOS for the majority (a) and minority (b) spins.

$c = 4.118 \text{ \AA}$. In this so-called DO₁₉ structure all the (001) planes, called A planes, show the same composition, Co₃Pt, and in this sense this structure is qualitatively equivalent to the preceding L₁₂ structure [5]. In the ferromagnetic phase F of the DO₁₉ structure, Co and Pt atoms have their magnetic moments oriented in the same direction. Actually we have also tried for this structure as well as for the other two structures the possibility with opposite orientations (the antiferromagnetic case), but during the self-consistent iteration

Table 1. Co₃Pt: a comparison between the paramagnetic (P) phase of DO₁₉ and the ferromagnetic (F) phases of DO₁₉, L1₂ and modified DO₁₉ (DO'₁₉) for various calculated quantities such as the total (per Co₃Pt) and partial (per atom) densities of states at the Fermi level $n^\sigma(E_F)$ and $n_\alpha^\sigma(E_F)$ (with $\alpha = \text{Co, Pt}$), the number of electrons for each l -orbital of Co and Pt origin $N_\alpha^\sigma(l)$ (with $l = s, p, d, f$), the charge variation ΔQ_α at Co and Pt atoms and the corresponding magnetic moment μ_α . On the lowest line we report the total energy E_{tot} per Co₃Pt. Let us remark that in the modified DO₁₉ structure we should differentiate between two types of Co atom; however, the numerical difference is so small that we prefer to show a mean value for the Co atom. Majority (minority) spins correspond to the up (down) direction.

	P DO ₁₉	F DO ₁₉	F L1 ₂	F DO' ₁₉
$n^\uparrow(E_F)$ (Ryd ⁻¹)	96.097	9.021	18.571	8.667
$n^\downarrow(E_F)$ (Ryd ⁻¹)	96.097	34.463	60.729	34.833
$n_{\text{Co}}^\uparrow(E_F)$ (Ryd ⁻¹)	28.111	2.223	4.083	0.950
$n_{\text{Co}}^\downarrow(E_F)$ (Ryd ⁻¹)	28.111	10.714	18.202	9.926
$n_{\text{Pt}}^\uparrow(E_F)$ (Ryd ⁻¹)	11.764	2.352	6.322	5.817
$n_{\text{Pt}}^\downarrow(E_F)$ (Ryd ⁻¹)	11.764	2.321	6.123	5.055
$N_{\text{Co}}^\uparrow(s)$	0.311	0.313	0.311	0.335
$N_{\text{Co}}^\downarrow(s)$	0.311	0.320	0.319	0.343
$N_{\text{Co}}^\uparrow(p)$	0.387	0.373	0.375	0.353
$N_{\text{Co}}^\downarrow(p)$	0.387	0.413	0.407	0.407
$N_{\text{Co}}^\uparrow(d)$	3.820	4.672	4.636	4.800
$N_{\text{Co}}^\downarrow(d)$	3.820	2.928	2.970	2.872
$N_{\text{Pt}}^\uparrow(s)$	0.415	0.402	0.405	0.391
$N_{\text{Pt}}^\downarrow(s)$	0.415	0.422	0.424	0.404
$N_{\text{Pt}}^\uparrow(p)$	0.413	0.375	0.384	0.311
$N_{\text{Pt}}^\downarrow(p)$	0.413	0.447	0.448	0.373
$N_{\text{Pt}}^\uparrow(d)$	4.041	4.317	4.288	4.331
$N_{\text{Pt}}^\downarrow(d)$	4.041	3.838	3.849	3.927
$N_{\text{Pt}}^\uparrow(f)$	0.075	0.072	0.077	0.045
$N_{\text{Pt}}^\downarrow(f)$	0.075	0.067	0.071	0.045
ΔQ_{Co}	0.037	0.020	0.018	0.123
ΔQ_{Pt}	-0.112	-0.060	-0.054	-0.370
$\mu_{\text{Co}}(\mu_B)$	0.0	1.698	1.626	1.602
$\mu_{\text{Pt}}(\mu_B)$	0.0	0.393	0.362	0.357
$E_F - \Gamma_1^\uparrow$ (Ryd)	0.720	0.725	0.725	0.725
$E_F - \Gamma_1^\downarrow$ (Ryd)	0.720	0.715	0.716	0.726
E_{tot} (Ryd)	-45 158.762	-45 158.817	-45 158.809	-45 158.791

this starting orientation automatically comes back to the F phase. In figure 3 we present the energy bands along some hcp high-symmetry directions in the paramagnetic P phase. The corresponding total DOS for both spin directions of the P phase is shown in figure 4. Furthermore figures 5(a) and 5(b) exhibit the total DOS in the F phase for majority and minority spins respectively. A direct comparison of the nearest-neighbour distances and the atomic radii for L1₂ and DO₁₉ structures is given in table 3.

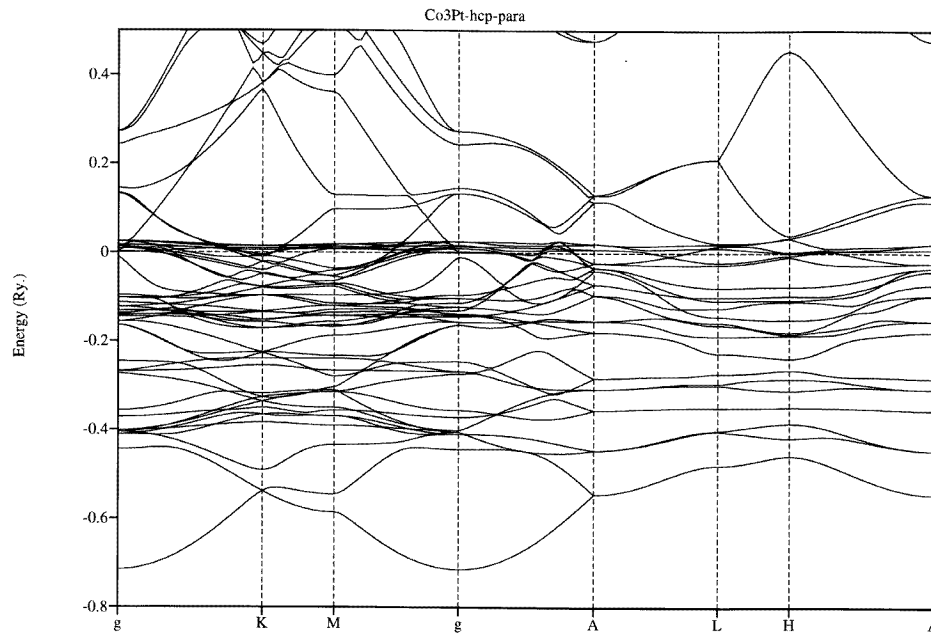


Figure 3. DO₁₉ Co₃Pt: the energy band dispersion along hcp high-symmetry directions in the paramagnetic phase.

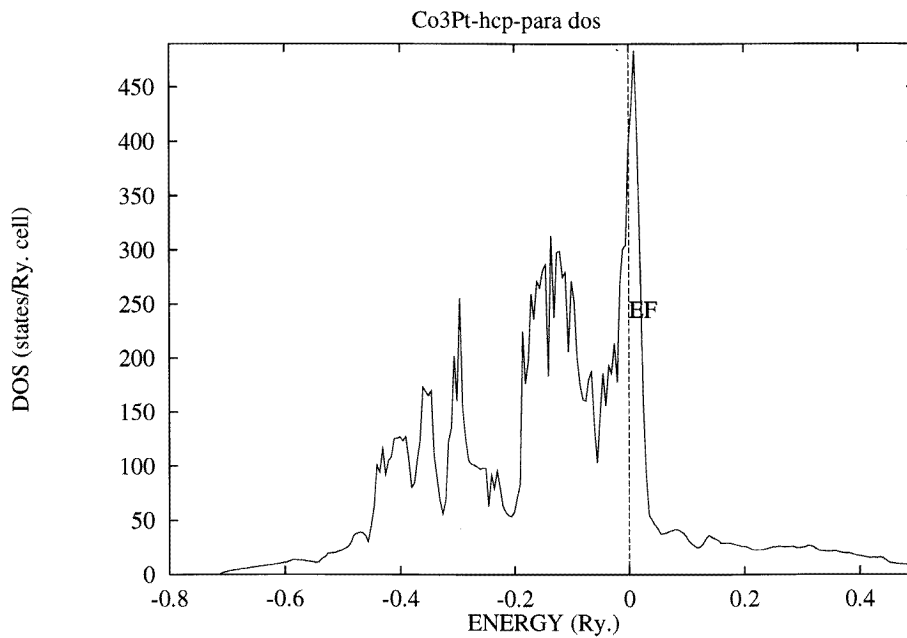


Figure 4. DO₁₉ paramagnetic Co₃Pt: the total DOS for both spin directions and per cell with Co₆Pt₂.

5. The modified DO₁₉ structure of Co₃Pt

As already explained in the introduction, we also performed a TB-LMTO band-structure calculation of the hcp structure of Co₃Pt, where all the Pt atoms are contained in the A

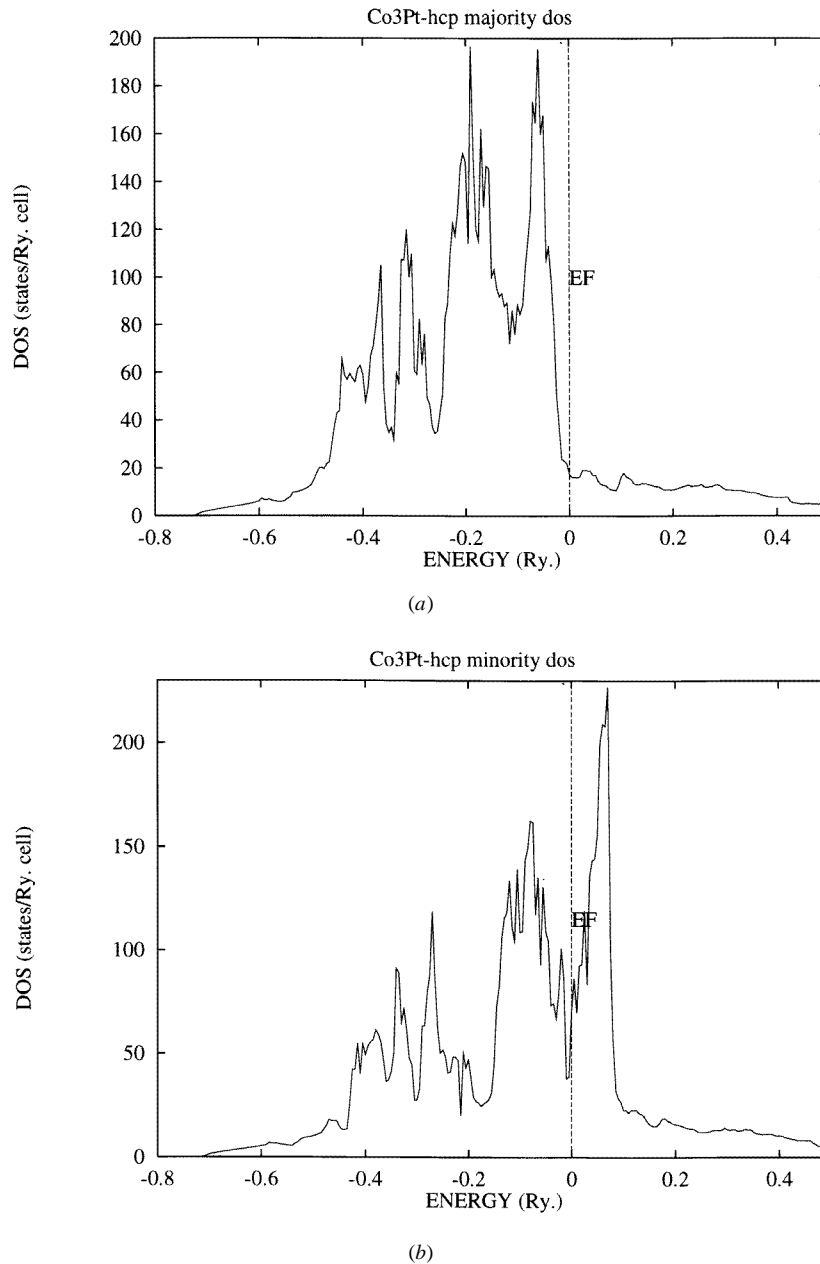
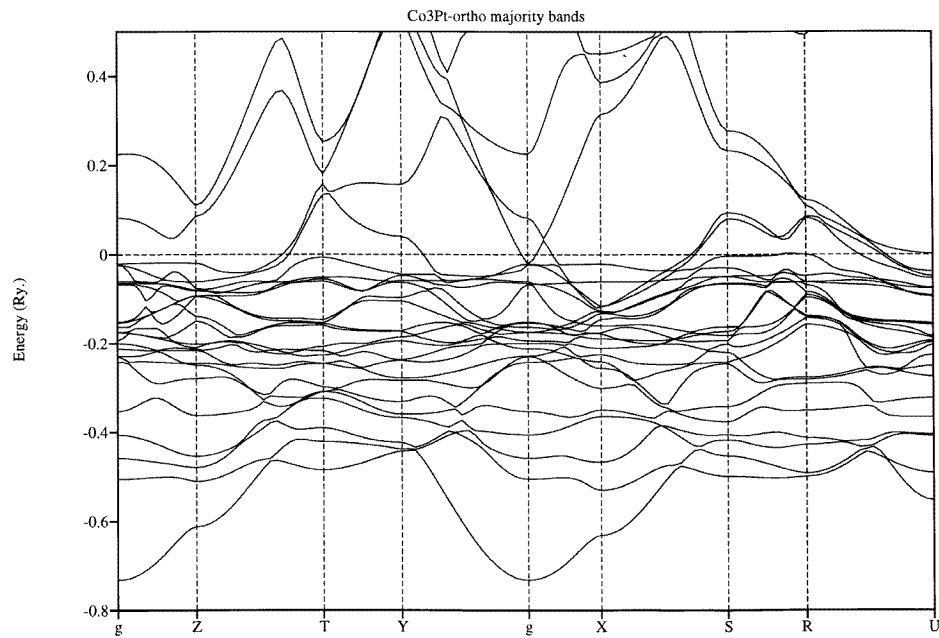
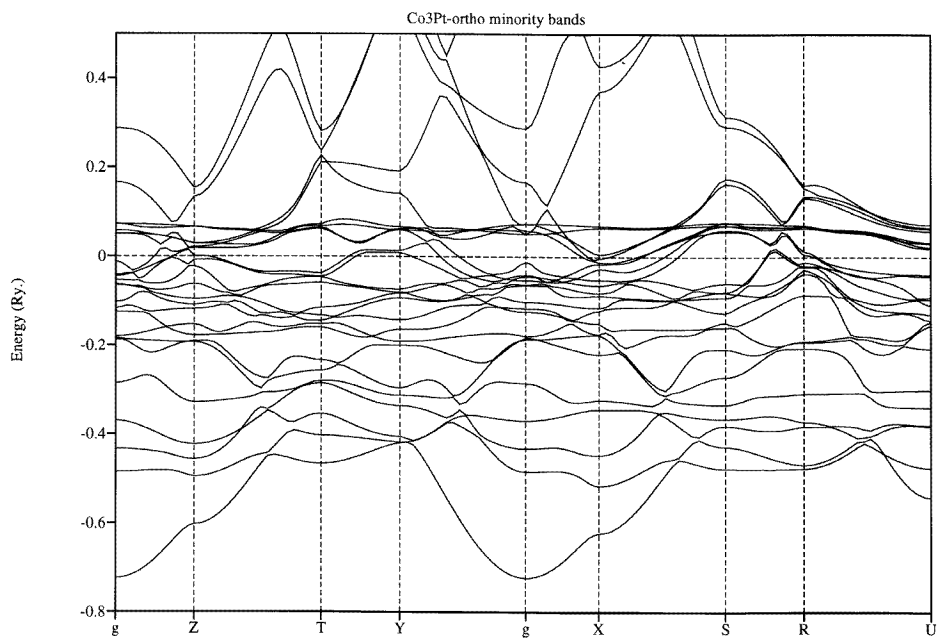


Figure 5. DO_{19} ferromagnetic Co_3Pt : the total DOS for majority (a) and minority (b) spins.

planes (two Pt atoms + two Co atoms in the upper half hexagonal unit cell) whereas only Co atoms appear in the B planes (four Co atoms in the lower half hexagonal unit cell); this ABAB structure is labelled DO'_{19} in the present paper. This particular phase, with eight atoms per unit cell as for the usual DO_{19} case, can also be represented in orthorhombic structure which will have the same bulk arrangement as the hcp one. The advantage of using orthorhombic structure is that now there are only four atoms per unit cell instead of eight



(a)



(b)

Figure 6. Modified DO₁₉ ferromagnetic Co₃Pt: the total DOS for majority (a) and minority (b) spins.

Table 2. Atomic positions of the hcp DO_{19} structure of Co_3Pt compounds with $x = 0.1627$, $a = b = 5.189 \text{ \AA}$ and $c = 4.196 \text{ \AA}$.

Two Pt sites	1/3	2/3	1/4
	2/3	1/3	3/4
Six Co sites	$1 - x$	$1 - 2x$	1/4
	$2x$	x	1/4
	$1 - x$	x	1/4
	x	$2x$	3/4
	$1 - 2x$	$1 - x$	3/4
	x	$1 - x$	3/4

Table 3. The lattice parameter a , the nearest-neighbour distance n.n.d., and the atomic radii $R_{\text{WS}}(\text{Co})$ and $R_{\text{WS}}(\text{Pt})$ of cobalt and platinum (in atomic units) for L_{12} and DO_{19} phases.

Structure	a (au)	n.n.d. (au)	$R_{\text{WS}}(\text{Co})$ (au)	$R_{\text{WS}}(\text{Pt})$ (au)
L_{12}	6.8620	4.8522	2.6335	2.8165
DO_{19}	9.7906	4.8953	2.6336	2.8166

as in the preceding case; hence the calculation time is much smaller as compared to that for hcp structure. The atomic positions for orthorhombic structure in the A plane are Pt(0, 0, 0) and $\text{Co}(\sqrt{3}a/4, a/4, 0)$ while in B plane there are only Co atoms at $(a/(2\sqrt{3}), 0, c/2)$ and $(-a/(4\sqrt{3}), a/4, c/2)$. The values of a and c are the same as given in the previous section (section 4). Hence the R_{WS} are also the same as for the DO_{19} structure. The corresponding total DOSs are reported for the majority (figure 6(a)) and minority (figure 6(b)) spins. Let us now discuss our numerical results for the various situations considered and compare the different phase structures of Co_3Pt compounds.

6. Discussion

From figures 1 and 3 it becomes obvious that the DOS at E_{F} will be quite important in the paramagnetic phase due to the flat bands at the Fermi level. Effectively, $n(E_{\text{F}}) = 96.097$ states $\text{Ryd}^{-1}/(\text{Co}_3\text{Pt spin})$ in the P DO_{19} structure (table 1) and in the other two structures the same situation is observed (but not reported in table 1). This high paramagnetic DOS at E_{F} , which is mainly due to d orbitals of Co, favours the existence of magnetism in Co_3Pt [19]. Also, according to our results, it is certain that the specific heat coefficients γ in the F phases of the various structures will be much smaller than those in P phases (i.e. $\gamma_{\text{P}} \gg \gamma_{\text{F}}$ whatever structure is considered). Moreover the total DOS of the F L_{12} phase at the Fermi energy ($=79.30$ states $\text{Ryd}^{-1}/\text{cell}$ from table 1) is close to the value found in [10] ($=82.96$ states $\text{Ryd}^{-1}/\text{cell}$ from their table 3) and hence the same remark is true for the γ -coefficient (see equation (2) and the discussion in [10]). For the F DO_{19} phase, the total DOS at E_{F} is 43.484 states $\text{Ryd}^{-1}/\text{cell}$ and γ is $1.88 \text{ mJ mol}^{-1} \text{ K}^{-2}$. The result is quite similar for the F DO'_{19} . However, there are no experimental γ -data available for Co_3Pt whatever phase is considered. Another general remark can be made on the basis of the charge-transfer behaviour— ΔQ of table 1: for all of the structures considered there is always a charge count ΔQ from Pt to Co atoms, whereas in [10] there is a small charge transfer from Co towards Pt in F L_{12} Co_3Pt , but, as already stated, this discrepancy is related to a different choice of R_{WS} . In DO'_{19} , ΔQ is the largest, i.e. each Pt atom loses $0.370e^-$ in favour of

Co, whereas in F DO₁₉ this charge transfer is almost one sixth of the preceding ($\simeq 0.060$) value—i.e. it is comparable to that of the L1₂ phase ($\simeq 0.054$). Finally, according to the total energy calculation results of table 1, the Co₃Pt system is the most stable in the F phase of the DO₁₉ structure. However, the difference ΔE between the total energies in F and P phases of DO₁₉ is about 0.75 eV, whereas the difference ΔE between the L1₂ and DO₁₉ phases is only about 0.1 eV. The hierarchy of the total energies of the various ferromagnetic phases is written as

$$E_{\text{tot}}(\text{DO}_{19}) < E_{\text{tot}}(\text{L1}_2) < E_{\text{tot}}(\text{DO}'_{19})$$

(the DO'₁₉ phase being less stable than the L1₂ phase).

Let us add a few more comments on the most stable F DO₁₉ structure. We observe that the occupied bands (figure 5) are almost the same as for the P phase (figure 4); the magnetic moment is then introduced due to a pronounced shift of the high-density peak in the P phase towards lower/higher-energy sides of E_F for majority/minority spins, respectively, in the F phase. The energy difference between those two peaks is about 1.77 eV. This value gives a rough estimate of the exchange parameter. In the DO₁₉ unit cell of Co₃Pt, the major ferromagnetic contribution comes from Co atoms which bear a magnetic moment $\mu = 1.698\mu_B/\text{atom}$ (table 1), comparable to the experimental values for CoPt: $\mu \simeq 1.7\mu_B/\text{atom}$ [20] and for pure metallic cobalt: $\mu \simeq 1.6\mu_B/\text{atom}$ [21]. Unfortunately the corresponding experimental data for Co₃Pt are also lacking. The Pt atoms are strongly spin polarized by the Co atoms and acquire an induced moment of $0.393\mu_B/\text{atom}$ (table 1). This last value agrees quite well with the number of holes (0.4) in the Pt 5d band. The only corresponding self-consistent band-structure calculation [10] gives the magnetic moments for the L1₂ phase of Co₃Pt: $\mu_{\text{Co}} = 1.64\mu_B$ and $\mu_{\text{Pt}} = 0.36\mu_B$. These values are almost the same as the ones we obtained, in spite of the fact that we have opposite charge transfer as compared to [10]. This confirms that the magnetic moment is mainly due to the local spin polarization.

7. Conclusion

In this paper we have presented the first *ab initio* calculation of the electronic structure of a new chemically ordered alloy of Co₃Pt in its DO₁₉ structure and its modified DO'₁₉ one, in comparison to the L1₂ structure. In the paramagnetic phase we find a high density of states at the Fermi level which favours the existence of a more stable ferromagnetic phase whatever the structure considered.

From total energy calculations we show that the ferromagnetic DO₁₉ phase is the most stable phase among all the various structures considered, but only at 0.1 eV below the energy of the ferromagnetic L1₂ phase. Moreover for the F DO₁₉ structure of Co₃Pt compounds the deduced magnetic moments on cobalt and platinum seem quite reasonable. Our results are encouraging and complementary to the experimental characterization of this new alloy phase deduced from MBE and not yet observed in the usual bulk alloys.

Acknowledgments

One of the authors (GM) would like to thank O K Andersen and O Jepsen for a one-week stay at MPI Stuttgart. Also, stimulating discussions with M Maret, V Pierron-Bohnes and M C Cadeville are gratefully acknowledged, as well as the communication of the Co₃Pt lattice parameters before publication. This work was partly supported by the European

Community Human Capital and Mobility Programme through contract No CHRX-CT93-0369. Finally, the authors would like to thank one of the referees for valuable suggestions.

References

- [1] Leroux C, Cadeville M C, Pierron-Bohnes V, Inden G and Hing F 1988 *J. Phys. F: Met. Phys.* **18** 2033
- [2] Massalski T 1990 *Binary Alloy Phase Diagrams* vol 2 (Metals Park, OH: American Society for Metals)
- [3] Sanchez J M, Moran-Lopez J L, Leroux C and Cadeville M C 1989 *J. Phys.: Condens. Matter* **1** 491
- [4] Harp G R, Weller D, Rabedeau T A, Farrow R F C and Toney M F 1993 *Phys. Rev. Lett.* **71** 2493
- [5] Maret M, Cadeville M C, Staiger W, Beaurepaire E, Poinsoot R and Herr A 1996 *E-MRS Spring Meeting (Strasbourg, 1995); Thin Solid Films* at press
- [6] Pearson W B 1967 *Handbook of Lattice Spacings and Structure of Metals and Alloys (International Series of Monographs in Metal Physics and Physical Metallurgy)* part 2, ed G V Raynor (Oxford: Pergamon)
- [7] Ducastelle F 1991 *Order and Phase Stability in Alloys* vol 3, ed F de Boer and D Pettifor (Amsterdam: North-Holland) p 145
- [8] Andersen O K and Jepsen O 1984 *Phys. Rev. Lett.* **53** 2571
- [9] Andersen O K, Pawlowska Z and Jepsen O 1986 *Phys. Rev. B* **34** 5253
- [10] Kootle A, Haas C and de Groot R A 1991 *J. Phys.: Condens. Matter* **3** 1133
- [11] Shirai M, Maeshima H and Suzuki N 1995 *J. Magn. Magn. Mater.* **140–144** 105
- [12] Lu Z W, Klein B M and Zunger A 1995 *Phys. Rev. Lett.* **75** 1320
- [13] Ujfalussy B, Szunyogh L and Weinberger P 1995 *Phys. Rev. B* **51** 12836
- [14] Von Barth U and Hedin L 1972 *J. Phys. C: Solid State Phys.* **5** 1629
- [15] Jepsen O and Andersen O K 1971 *Solid State Commun.* **9** 1763
- [16] Lehman G and Taut M 1972 *Phys. Status Solidi b* **54** 469
- [17] Parlebas J C, Christensen N E, Runge E and Zwickyngl G 1988 *J. Physique Coll.* **49** C8 753
- [18] Parlebas J C 1989 *J. Physique* **50** 957
- [19] Stoner E C 1939 *Proc. R. Soc. A* **169** 339
- [20] Van Laar B 1964 *J. Physique* **25** 600
- [21] Ahuja R, Auluck S, Johansson B and Khan M A 1995 *J. Magn. Magn. Mater.* **140–144** 89